NASA TECHNICAL NOTE

NASA TN D-3307

c. 1

NASA TN D-3307

HIGH-POWER-LEVEL TEMPERATURE CONTROLLER FOR SPACE FLIGHT APPLICATIONS

by William T. Harrigill, Jr., and L. Jack Smith

Lewis Research Center
Cleveland, Ohio

NATIONAL AERONAUTICS AND SPACE ADMINISTRATION • WASHINGTON, D. C. • MARCH 1966

HIGH-POWER-LEVEL TEMPERATURE CONTROLLER

FOR SPACE FLIGHT APPLICATIONS

By William T. Harrigill, Jr., and L. Jack Smith

Lewis Research Center
Cleveland, Ohio

NATIONAL AERONAUTICS AND SPACE ADMINISTRATION

For sale by the Clearinghouse for Federal Scientific and Technical Information
Springfield, Virginia 22151 – Price $0.35

HIGH-POWER-LEVEL TEMPERATURE CONTROLLER FOR SPACE FLIGHT APPLICATIONS

by William T. Harrigill, Jr., and L. Jack Smith

Lewis Research Center

SUMMARY

A solid-state duty-cycle controller was developed and tested that is capable of controlling loads up to 8 kilowatts and 1250° F. The load can be held to within ±10° F of the design temperature while the controller is operating under simulated space flight conditions. The prototype model is capable of storing the heat losses involved in a short-duration (10-min) flight. The system operates from an 80-volt direct-current supply with an efficiency of 98 percent. The temperature sensor used is a resistance thermometer. The design of the system includes modular construction techniques, which make it readily adaptable to a variety of load and temperature requirements.

INTRODUCTION

The design of automatic controllers for maintaining test conditions in experiments is often complicated by the variety of requirements imposed on the controller. For experiments to be carried out in space, these requirements will become even more restrictive. The work described in this report was the result of requirements posed by an experiment to measure the zero-gravity performance of boilers and capacitators for Rankine cycle space power systems. Chief factors affecting this design were temperature regulation, power level, power source (battery packs), efficiency, and reliability.

Temperature regulation to ±10° F at a boiler outlet temperature of 1250° F was the desired goal for the controller. Factors affecting this regulation include changes in heating load, supply voltage changes due to battery discharge, temperature sensor drift, and the characteristics of both the controller and the heaters to be controlled.

The power levels of the heaters ranged from about 8000 watts for the boiler to 1000 watts for the smaller heaters. Compromises between battery pack voltage and boiler design led to requirements for circuitry capable of controlling an average current of 100 amperes. The availability of components for these current levels and such factors as efficiency and reliability further complicated this design problem.

Efficiency and reliability considerations are, of course, inherent in any

rocket-vehicle-borne experiment. Efficiency is of concern to minimize the weight of battery packs and also of any heat sinks required to absorb controller losses during the space experiment. Reliable operation during launch and in the space environment called for solid-state circuitry.

High power levels, which are relatively new to space experiments, are inherent to Rankine cycle space power systems research. As such research continues, similar control requirements are expected to arise for space experiments for which knowledge gained from this controller will be applicable.

A type of controller well suited to high-power, high-efficiency requirements is the duty-cycle controller. In this device the average power is controlled by varying the ratio of on time to off time of a constant-voltage rectangular wave. The high efficiency of this system results from the fact that the power controlling portion of the system is a switch, which turns power fully on and then fully off. However, since the power is continuously controlled (averaged over 1 duty cycle), this type of controller has a proportional control characteristic, free from dead band and temperature cycling inherent in on-off controllers.

Duty-cycle control has been used extensively in temperature controllers for ground-based applications where alternating-current power is controlled. Such a system is described in reference 1. Another ground-based application of this technique is in motor speed control, where continuous control and high efficiency are desired. Reference 2 describes such applications. A space flight application of duty-cycle control is described in reference 3. This is a high-efficiency direct current to direct current converter with regulated output voltage.

The design of high-power solid-state switching circuits operating from direct-current supplies presents a problem. Silicon controlled rectifiers (SCR) have recently become available for switching such high currents. The control circuits to ensure reliable turn-off of these elements when the circuits are operating from direct-current power sources can become complex. This is particularly true if electrical noise is likely to be present in the power supply. Such troublesome noise arises from switching transients as other loads on the vehicle are operated. The solution to this noise problem is discussed in detail.

The controller described herein represents a successful mating of this well known duty-cycle technique with a reliable high-power direct-current switching circuit to produce an all-solid-state controller that can be used in flight applications. The advantage gained from this work is that the proportional gain characteristic and the high efficiency of duty-cycle control can be applied to flight-experiment control problems requiring precise, continuous control of high power loads driven from direct-current power sources. A further advantage of this particular controller is its ready adaptability to a variety of load characteristics. This is achieved through the use of a temperature-to-duty-cycle converter capable of driving SCR switching circuits matched to a variety of power levels.

The extent of this work has been limited to the design and testing of a prototype system capable of meeting the requirements outlined for the heater. Testing of the system has included demonstration of reliable operation in the presence of simulated electrical noise on the vehicle power supply. The effects of variation of circuit temperature and power supply voltage were also measured.

SYMBOLS

G defined by eq. (3) in appendix

K_L slope of load characteristic curve

K_1 steady-state transfer function of sensor

K_2 steady-state transfer function of resistance-to-duty-cycle converter

R_H heater resistance

ΔT change in temperature from set point

T_o design temperature (set point)

V_B switching circuit supply voltage

V_{Bo} design value of switching circuit supply voltage

W_D average power delivered to load

W_L average power required by load

W_o design average power delivered to load

W_p peak power (power at 100 percent duty cycle) delivered by controller

W_{po} design peak power

ΔW_x defined by eq. (12) in appendix

η duty cycle

η_o design duty cycle

Φ angle between horizontal axis and load characteristic curve (figs. 8 and 9)

θ angle between horizontal axis and power delivered curve (figs. 8 and 9)

DESCRIPTION OF CONTROL SYSTEM

Principle of Operation

Figure 1 shows a block diagram of the temperature control system. As shown in this diagram, the system consists of a sensor, an electrical bridge, a control circuit, and a switching circuit.

The sensor is a resistance thermometer which is connected as one arm of the bridge. The bridge, the control circuit, and the switching circuit act as a resistance-to-duty-cycle converter. It should be noted that the control circuit in combination with a low-power switching circuit such as a multivibrator can be used as a resistance-to-duty-cycle converter for special-purpose data handling. This combination was successfully operated in this manner at clock frequencies up to 3000 hertz without modification of the circuit. The resistance-to-duty-cycle converter generates a square wave of voltage with a constant repetition rate whose amplitude is either zero or power supply voltage and whose ratio of on to off time (duty cycle) is inversely proportional to a change in the resistance of the sensor about a preselected value. By varying the duty cycle of this wave, the average power delivered to the heater (and, in turn, the temperature of the heater) is controlled.

The correct duty cycle is achieved in the following manner. At a predetermined temperature (set point) the resistances of the bridge are selected such that the bridge is balanced. The heater is switched off at the beginning of each duty cycle, and the bridge is electrically forced to an unbalanced condition by the control circuit. This condition is then changed by the control circuit in a sequence of steps during the remainder of the cycle. As the bridge passes through balance, the bridge output signal reverses polarity and causes power to the heater to be turned on for the rest of the cycle. If the temperature of the heater deviates from the set point, the change in sensor resistance causes the bridge to pass through balance at a different step in the cycle. The resultant change in duty cycle adjusts the average power in a direction which tends to restore the heater to its design temperature. For this new condition, however, the heater must stabilize at a temperature slightly different from the set point in order to establish the new required duty cycle. The range of heater temperatures between the temperature that would be established with a 0-percent duty cycle and the temperature for a 100-percent duty cycle constitutes the control range of the system. If it becomes necessary to exceed the control range temporarily, as would be the case for a large step change in heater load, the power to the heater will remain fully on or off until the temperature returns to the control range.

Control Circuit

The primary function of the control circuit is to detect when the bridge passes through balance and subsequently generate a power turn-on signal. The control circuit (fig. 2) and, consequently, the entire controller are driven by a free-running asymetrical multivibrator (clock) that generates 300-microsecond pulses at the rate of 160 per second. Sixteen of these pulses are

provided each duty cycle, and a basic duty-cycle rate of 10 hertz is established (line 1, fig. 2).

These clock pulses serve three purposes. First, the pulses are used to power the bridge circuit. Second, the clock drives a binary counter which, together with a resistance sequencer, changes the balance of the bridge. Third, the clock pulse is used to gate the output of the control circuit.

The main purpose for pulsing the bridge was to permit the use of a simple alternating-current coupled amplifier (fig. 2) at the output of the bridge rather than a low-level chopper system or a complicated direct-current amplifier. This technique of pulsing bridge circuits has been used for quite some time. As pointed out in references 4 and 5, this scheme is normally used to obtain large output signals while dissipating a minimum of power in the bridge circuit. This, however, was not the primary reason for its use in this control system.

Since the bridge is energized only during the 300-microsecond clock pulse, the output signal will appear as a pulse train as shown in the second line of figure 2. When the bridge is unbalanced at the beginning of the cycle, the output signal is negative and becomes more positive for each of the succeeding 16 steps. A turn-on signal will be developed at the input of the switching circuit when the bridge output becomes positive. The switching circuit switches on (line 4, fig. 2) because of the first of these signals and remains on until the end of the cycle. The remaining information in figure 2 will be discussed in the description of the gate.

The bridge balance is changed in discrete steps by the resistance sequencer (figs. 2 and 3) rather than in a continuously variable manner. This technique is reported in reference 6, where capacitance is the electrical quantity to be varied, and in reference 7, where resistance is varied. The resistance sequencer changes the bridge balance in 16 equal steps by varying the effective resistance of one arm of the bridge. This is accomplished by connecting a known resistor in series with a diode from the output of each stage of a four-stage binary counter to the junction of resistors 5 and 6 in the bridge circuit. As the counter is triggered by each clock pulse to a new position, a different parallel combination of resistances will be switched across resistor 5. This process provides a total of 16 combinations of resistances. When the values of these resistances (R_1, R_2, R_3, R_4) are weighted in a binary (8, 4, 2, 1) manner, the effective resistance will be changed in almost equal increments provided the total change is small in comparison to the bridge resistance R_5.

The description of the resistance sequencer can be summarized by stating that it acts as a variable resistor with a range equal to the total change in the combinations of R_1, R_2, R_3, R_4, and R_5 and is stepped through its range (in equal increments) once each duty cycle by the clock. Sixteen steps were selected for the prototype to assure a temperature detection of less than 1° F.

When the variable resistor and the sensor are connected in the bridge, a change in sensor resistance and, in turn, a change in heater temperature are

detected at the output of the bridge. A correction in duty cycle then takes place as discussed in the section Principles of Operation. Thus, it can be seen that the control range of the system is in effect set by the range of the variable resistor. The selection of the control range of the prototype (±7° F) is based on two conditions: first, that the temperature of the boiler will remain within the required overall accuracy of control (±10° F) for a 100-percent change in duty cycle; and second, that readily available resistance can be used to implement the resistance sequencer.

From figure 2, it can be seen that a gate is used between the amplified bridge output and the switching circuit. The purpose of this gate is to eliminate the effects of voltage transients generated when the bridge is energized. These transients are caused by the fast rise and fall of the clock pulse. To prevent these signals from appearing at the input of the switching circuit, the gate is opened 200 microseconds after the start of each clock pulse for a period of 10 microseconds. In this way a turn-on signal will appear (line 3, fig. 2) only during a transient-free interval of each clock pulse.

The activating signal for this gate (line 5, fig. 2) is obtained by first delaying the clock pulse with a monostable multivibrator and then reducing its effective width by a differentiating circuit.

Another function of the control circuit is to provide a reset signal to the switching circuit at the beginning of each cycle. This is accomplished by differentiating the positive going voltage that occurs at the output of the last stage of the binary counter every 16th clock pulse. This pulse establishes the duty-cycle rate of the prototype at 10 hertz. The duty-cycle frequency of 10 hertz was selected high enough to reduce the thermal ripple to a value below an acceptable level.

Switching Circuit

The function of the switching circuit is to convert the previously described turn-on and turn-off signals generated in the control circuit into a square wave of voltage. This voltage is then applied to the heater to complete the last step in the resistance-to-duty-cycle conversion. The switching circuit is a self-holding switch that connects the direct-current power supply to the heater when activated by the turn-on signal and remains closed until opened by the reset signal.

Because of the large current handling ability required by this operation (200 A for the prototype), a circuit utilizing an SCR as the primary switching element is ideally suited. An SCR switching circuit commonly used for this purpose is shown in figure 4 and is fully described in reference 1. In this circuit, voltage is applied to the load by firing SCR 1. The shunt condenser is charged through resistor A during the time that voltage is applied to the load. The voltage developed across the condenser is then used to back bias SCR 1 and turn it off when SCR 2 is fired by a reset signal. This same techique is used to turn off SCR 2 when SCR 1 is again triggered on. This

conventional circuit, suitable for most applications, has two characteristics which make it undesirable in its present form for this application. First, the efficiency of the circuit is reduced by dissipating power in resistor A during the off time of the cycle (when SCR 2 is conducting). If the value of resistance A, R_A, is made large, this loss will be minimized, but an upper limit is placed on its value by the time constant R_AC. Resistance A must be chosen small enough to allow the condenser to collect sufficient charge to supply SCR 1 with a back bias voltage. This power loss is incompatible with the high efficiency requirement for this controller.

The second undesirable characteristic of this conventional circuit is that, if SCR's 1 and 2 are simultaneously triggered on by a noise pulse when the condenser has insufficient back bias voltage to turn one or the other off, both SCR's will remain on. This causes power supply voltage to be permanently switched to the heater.

A modified circuit which eliminates these problems is shown in figure 5 along with a sequence diagram of one cycle of operation.

The operation of this circuit is similar to that of the conventional circuit. Prior to the start of the cycle the condition of the circuit is as shown in the diagram. The voltage across the heater is V_B (line 1, fig. 5), the transistor is conducting because of the bias voltage supplied from the control circuit (line 2, fig. 5), the condenser is charged with the polarity shown in the circuit diagram and line 3, and SCR's 2 and 3 are not conducting.

At the start of the cycle SCR's 2 and 3 are switched on by the reset signal and a back bias voltage cuts SCR 1 off and thus disconnects the supply voltage from the heater. At the same time, the bias voltage is removed from the base of the transistor which opens the conducting path through resistor A. SCR 2 will remain in the conducting state until the condenser reduces its current below the minimum required holding current by charging to the opposite polarity of voltage. Although SCR 3 will continue to conduct through resistor B and the heater resistor, less than 1 percent of the supply voltage will be developed across the heater from this source.

The next sequence of events takes place at the beginning of the third step in the cycle. Here the transistor is made to conduct by supplying base voltage (line 2, fig. 5) from the binary decoder (fig. 2). When this happens, the capacitator is placed in series with resistors A and B, and since resistor A is smaller in value (15 ohms) than resistor B (50 ohms), a negative voltage is placed at the anode of SCR 3 (line 4). This negative voltage forces SCR 3 off and allows the capacitator to recharge to its original polarity (as shown in the circuit diagram) during the remainder of the cycle. Line 1 of the sequence diagram shows SCR 1 firing some time during the remainder of the cycle. If SCR 1 is turned on during the first two steps of the cycle, SCR's 2 and 3 will be immediately shut off and the rest of the cycle will follow the same procedure as described previously.

The major features of this modification are the following:

(1) The insertion of a transistor eliminates the unnecessary dissipation of power in resistor A that was present in the conventional circuit (fig. 4) by

never allowing SCR 2 to conduct current directly through resistor A. Only the small power loss involved in charging the capacitator is left. The result is an increase in circuit efficiency. An estimate shows that for the prototype model operating at its design load (8000 W) the conventional circuit should operate with an efficiency of 80 to 90 percent while the modified circuit operates with an efficiency of 98 percent.

(2) The possibility of a complete circuit failure is also removed by the addition of the transistor. If the SCR's are switched on from a noise pulse at a time when there is insufficient back biasing voltage across the capacitator, both of these SCR's cannot remain on since the transistor will open the conducting path through resistor A each cycle. This allows the capacitator to charge through SCR's 2 and 3 and the heater resistance, shut off, and resume normal operation.

(3) SCR 3 and resistor B are added to the circuit in order to give the capacitator the majority of the cycle (14/16) in which to recharge. In the conventional circuit this recharge time could be as short as 1/16 cycle. With this increased charging time allowed, the charging current can be reduced to within the range of allowable collector currents found in commercial silicon transistors.

SYSTEM PERFORMANCE EVALUATION

A series of tests was conducted to check the performance of the control system while it was operating under simulated electrical and thermal space flight conditions. These tests and the equipment used to conduct these tests are described in the following discussion.

Equipment

A simulated load was fabricated by winding stainless steel tubing into a helix. The helix acted as an electrical heating coil, and power was supplied by connecting the ends of the helix directly to the output of the switching circuit. This power was dissipated as heat loss to the surrounding atmosphere. A resistance thermometer was mounted on the surface of the tube.

Load temperature was measured by a thermocouple mounted on the tube. Probable error in the load temperature was estimated as ±0.7 percent for absolute values and ±0.2 percent (±2.5° F) for changes in temperature.

Power was supplied to the switching circuit from a supply capable of delivering over 200 amperes at 100 volts with 14 percent ripple. A regulated low-voltage supply maintained the control circuit at its design voltage of 5.5 volts.

For short-duration (10-min) tests a $3\frac{1}{2}$-pound aluminum block was used as a heat sink for SCR 1, and resistors A and B had sufficient mass to absorb their power dissipation without excessive temperature rise.

Steady-State Transfer Function Test

Three steady-state transfer functions which are used to calculate the effect that a change in both load and switching-circuit supply voltage has on the load temperature were experimentally verified. These terms are given in the appendix along with the equations used in these calculations.

The equation which is used to calculate the effect of a load change is given in the appendix as

$$\Delta T = \frac{\Delta W_o}{G - K_L} \tag{11}$$

The steady-state values of K_1, K_2, and K_L were measured as 0.426 ohm per $^{\circ}F$, -0.169Δ duty cycle per ohm, and 18 watts per $^{\circ}F$, respectively. From the values of K_1 and K_2, G was calculated to be -1152 watts per $^{\circ}F$. When the values of G and K_L are used in the preceding equation, it is found that a variation of $\pm 0.7^{\circ}$ F will occur for a $\pm$10-percent change in load for the design values of $R_H = 0.4$ ohm, $V_{B_o} = 80$ volts, and $W_O = 8000$ watts.

Switching-Circuit Evaluation Test

The equation showing the effect of a switching-circuit supply voltage change is given in the appendix as

$$\Delta T = \frac{\eta_o\left(2V_{B_o}\,\Delta V_B + \Delta V_B^{\,2}\right)}{R_H\left[K_L - \dfrac{G\left(V_{B_o} + \Delta V_B\right)^2}{V_{B_o}^{\,2}}\right]} \tag{28}$$

Figure 6 shows the curve obtained from this equation along with the curve obtained experimentally by operating the control system at design conditions and varying only the switching-circuit supply voltage.

As shown in figure 6, if the system remains within its control range, the load will vary from 1° to -7° F about the set point for a voltage variation of 5 to -25 volts about V_{B_o}. However, if the supply voltage is reduced to a value where a 100-percent duty cycle is established (approximately 55 V), large variations will result from small changes in voltage, since the temperature can no longer be corrected by a change in duty cycle.

Control-Circuit Environmental Test

The control circuit was evaluated by controlling the load temperature with

the complete system but exposing only the control circuit to environmental test conditions. The temperature of the control circuit was varied in steps from -20° to 170° F. At each of these temperatures the control-circuit supply voltage was varied ± 10 percent about its design point. For each of these conditions the temperature of the load was measured. The ambient pressure was 0.3 millimeter of mercury throughout the test. The data plotted in figure 7 show that all of the load-temperature variations remained within the probable error band of the thermocouple measuring system.

Simulated Flight Test

The simulated flight test demonstrated that the controller could successfully maintain set point temperature under simulated pressure and temperature flight conditions. The entire system (excluding the load) was operated at a pressure of 0.3 millimeter of mercury and a temperature of 90° F for a period of 14 minutes. During this time the load temperature did not vary by a measurable amount. The SCR 1 heat sink and resistors A and B proved to be adequate for the prototype. The stud temperature of SCR 1 remained below its maximum operating value of 250° F. The resistors reached a temperature of 390° F.

Noise Test

The noise test experimentally confirmed that the previously described modified switching circuit will not be disabled when falsely triggered by an electrical noise pulse. An analysis of the circuit shows that a temporary interruption in normal operation can occur when SCR's 2 and 3 are misfired after the first two steps of the cycle or when the load SCR (SCR 1) is misfired. To prove that the switching circuit would recover when SCR's 2 and 3 were misfired, external trigger signals were applied to these SCR's. Both were fired separately and then simultaneously. In order to allow ample time for recovery between firings, the signals were synchronized with the clock in the control system and applied every fourth cycle. No tests were made for the obvious condition where SCR 1 is inadvertently triggered on.

The output voltage of the switching circuit and the external trigger signal were observed on a dual beam oscilloscope. These waveforms showed that the circuit resumes normal operation within 1 cycle after a malfunction occurs.

Efficiency Test

Power measurements were taken of the system while it operated at its design load of 8000 watts in order to determine an overall system efficiency. The average power dissipated in SCR 1 and resistors A and B was 163 watts. Power dissipation in all other components was negligible. An efficiency of 98 percent (excluding internal voltage supply losses) was calculated from these measurements.

CONCLUDING REMARKS

The preceding sections of this report describe a temperature controller designed to meet a set of requirements which include not only accurate control of large power levels but reliable operation in a space flight vehicle. The design is based on duty-cycle control which combines high efficiency with proportional control characteristics. Implementation of the system includes a special high-power switching circuit free from failure due to electrical noise.

The evaluation of the prototype controller can be summarized as follows:

(1) The total deviation in temperature of an 8000-watt load is held to within 5° F while the control circuit is exposed to an ambient temperature change from -20° to 170° F and the control-circuit supply voltage is varied ± 10 percent.

(2) A variation of 5 to -25 volts in the switching-circuit voltage causes a 1° to -7° F change in load temperatures.

(3) The system controls to within $\pm 0.7^\circ$ F of the set point temperature for thermal load changes of ± 10 percent.

(4) Simulated electrical noise transients do not appreciably affect the performance of the system.

This basic model can be applied to temperature problems which require operation from a direct-current supply with high efficiency under a wide variation of ambient temperature. Because of its modular construction, the system is easily tailored to meet a variety of temperature control requirements without redesign. For example, a new set point temperature can be selected by changing the bridge resistances. The control range can be modified by changing the resistances in the resistance sequencer. A wide range of loads can be accommodated by adjusting the switching-circuit supply voltage and making minor component changes.

Lewis Research Center,
National Aeronautics and Space Administration,
Cleveland, Ohio, November 3, 1965.

APPENDIX - STEADY-STATE TRANSFER FUNCTIONS

The steady-state transfer functions of the system are defined by the following equations:

$$K_1 = \frac{\Delta R}{\Delta T} \tag{1}$$

$$K_2 = \frac{\Delta \eta}{\Delta R} \tag{2}$$

$$G = K_1 K_2 W_{po} \tag{3}$$

When $V_B = V_{B_o}$

$$G = \frac{\Delta W_D}{\Delta T} \tag{4}$$

Since

$$W_{po} = \frac{V_{B_o}^2}{R_H} \tag{5}$$

$$G = \frac{K_1 K_2 V_{B_o}^2}{R_H} \tag{6}$$

Figure 8 shows a plot of the power delivered against load temperature superimposed on a portion of the characteristic curve of the load. Since the power delivered to the load must be equal to the power required by the load, the intersection of these two curves gives the stable operating point of the control system. The following equation, showing the relation between a load change ΔW_o and a change in load temperature, is derived from figure 8:

$$\Delta W_D = G\,\Delta T \tag{7}$$

where $G = \text{tangent } \theta$.

$$\Delta W_L = \Delta W_o + \Delta T K_L \tag{8}$$

where $K_L = \text{tangent } \Phi$. Since

$$\Delta W_L = \Delta W_D \tag{9}$$

$$G\,\Delta T = \Delta W_o + \Delta T K_L \tag{10}$$

$$\Delta T = \frac{\Delta W_o}{G - K_L} \tag{11}$$

Figure 9 is similar to figure 8 except that the peak power is varied while the load is held constant. The following equation, describing the relation between a change in load temperature and a change in switching-circuit voltage, is derived from figure 9:

$$\Delta W_x = \frac{\Delta W_p}{W_p} W_D \tag{12}$$

Since

$$W_D = W_o + \Delta W_D \tag{13}$$

$$\Delta W_x = \frac{\Delta W_p}{W_p}\left(W_o + \Delta W_D\right) \tag{14}$$

or

$$\Delta W_x = \Delta W_D - G\ \Delta T \tag{15}$$

Setting equation (14) equal to (15) results in

$$\Delta W_D = \frac{\frac{W_o}{W_p} \Delta W_p + G\ \Delta T}{1 - \frac{\Delta W_p}{W_p}} \tag{16}$$

$$\Delta W_L = \Delta T K_L \tag{17}$$

Since

$$\Delta W_L = \Delta W_D \tag{18}$$

$$\Delta T K_L = \frac{\frac{W_o}{W_p} \Delta W_p + G\ \Delta T}{1 - \frac{\Delta W_p}{W_p}} \tag{19}$$

Solving for ΔT yields

$$\Delta T = \frac{W_o \frac{\Delta W_p}{W_p}}{K_L\left(1 - \frac{\Delta W_p}{W_p}\right) - G} \tag{20}$$

Since

$$\frac{W_o}{W_{po}} = \eta_o \tag{21}$$

and

$$W_p = W_{po} + \Delta W_p \tag{22}$$

$$\Delta T = \frac{\eta_o \Delta W_p}{K_L - G\left(1 + \frac{\Delta W_p}{W_{po}}\right)} \tag{23}$$

$$\Delta W_p = \frac{V_B^2 - V_{B_o}^2}{R_H} \tag{24}$$

If

$$V_B = V_{B_o} + \Delta V_B \tag{25}$$

$$\Delta W_p = \frac{2V_{B_o} \Delta V_B + \Delta V_B^2}{R_H} \tag{26}$$

$$W_{po} = \frac{V_{B_o}^2}{R_H} \tag{27}$$

Substituting the values of ΔW_p and W_{po} into equation (23) gives

$$\Delta T = \frac{\eta_o\left(2V_{B_o} \Delta V_B + \Delta V_B^2\right)}{R_H\left[K_L - \frac{G\left(V_{B_o} + \Delta V_B\right)^2}{V_{B_o}^2}\right]} \tag{28}$$

REFERENCES

1. Anon: Silicon Controlled Rectifier Manual. 2nd ed., General Electric Company (Auburn, N.Y.), 1961.

2. Walston, Joseph A.; and Miller, John R., eds.: Transistor Circuit Design. McGraw-Hill Book Co., Inc., 1963, pp. 475-480.

3. McLeod, James A.: One-Step Converter for Ease of Voltage Conversion. IEEE Intern. Conv. Record, vol. 12, pt. 7, 1964, pp. 241-245.

4. Sanders, Newell D.; and Brodie, George H.: Application of Pulse Techniques to Strain Gages. NACA RM E54B08, 1954.

5. Stein, Peter K.: Pulsing Strain-Gage Circuits. Instr. Control Systems, vol. 38, no. 2, Feb. 1965, pp. 128-134.

6. Blanchard, Robert L.; and Sherburne, Arthur E.: A Digital Capacitance System for Mass, Volume, and Level Measurements of Liquid Propellants. Paper No. 2639-62, ARS, Nov. 1962.

7. Semyan, John : Digital Ohmmeter. NASA TN D-2003, 1964.

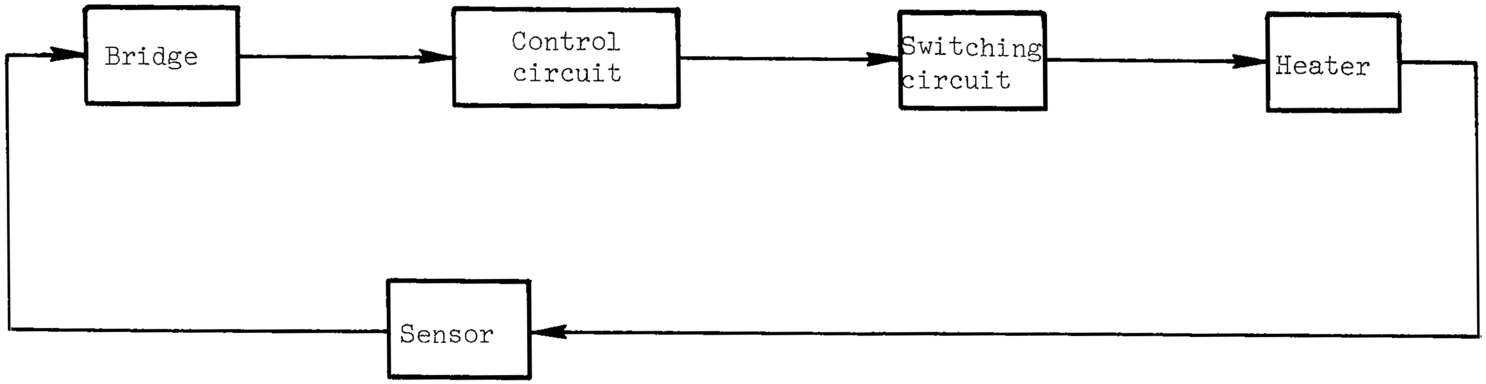

Figure 1. - Block diagram of temperature controller.

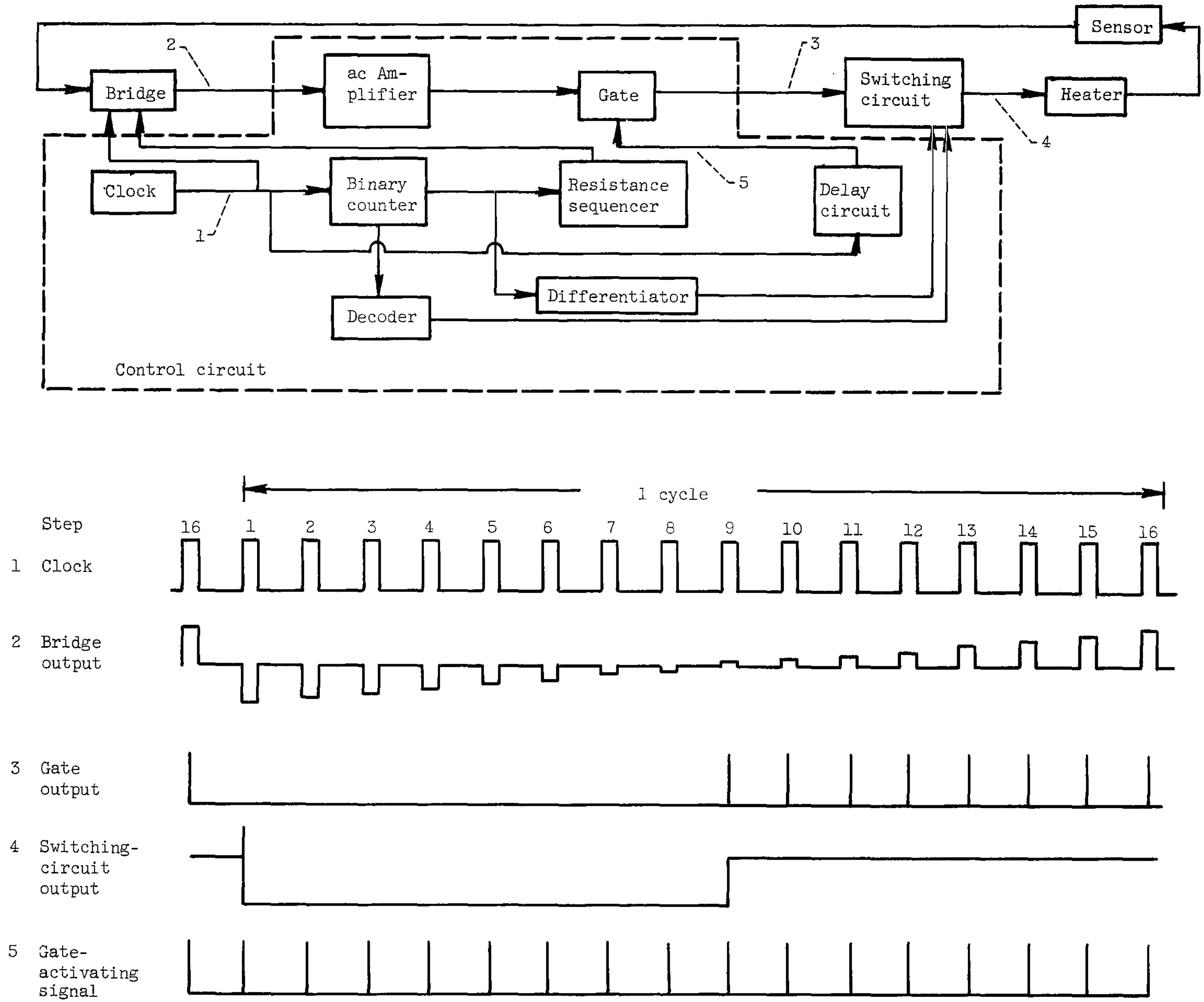

Figure 2. - Temperature controller block diagram and time sequence diagram.

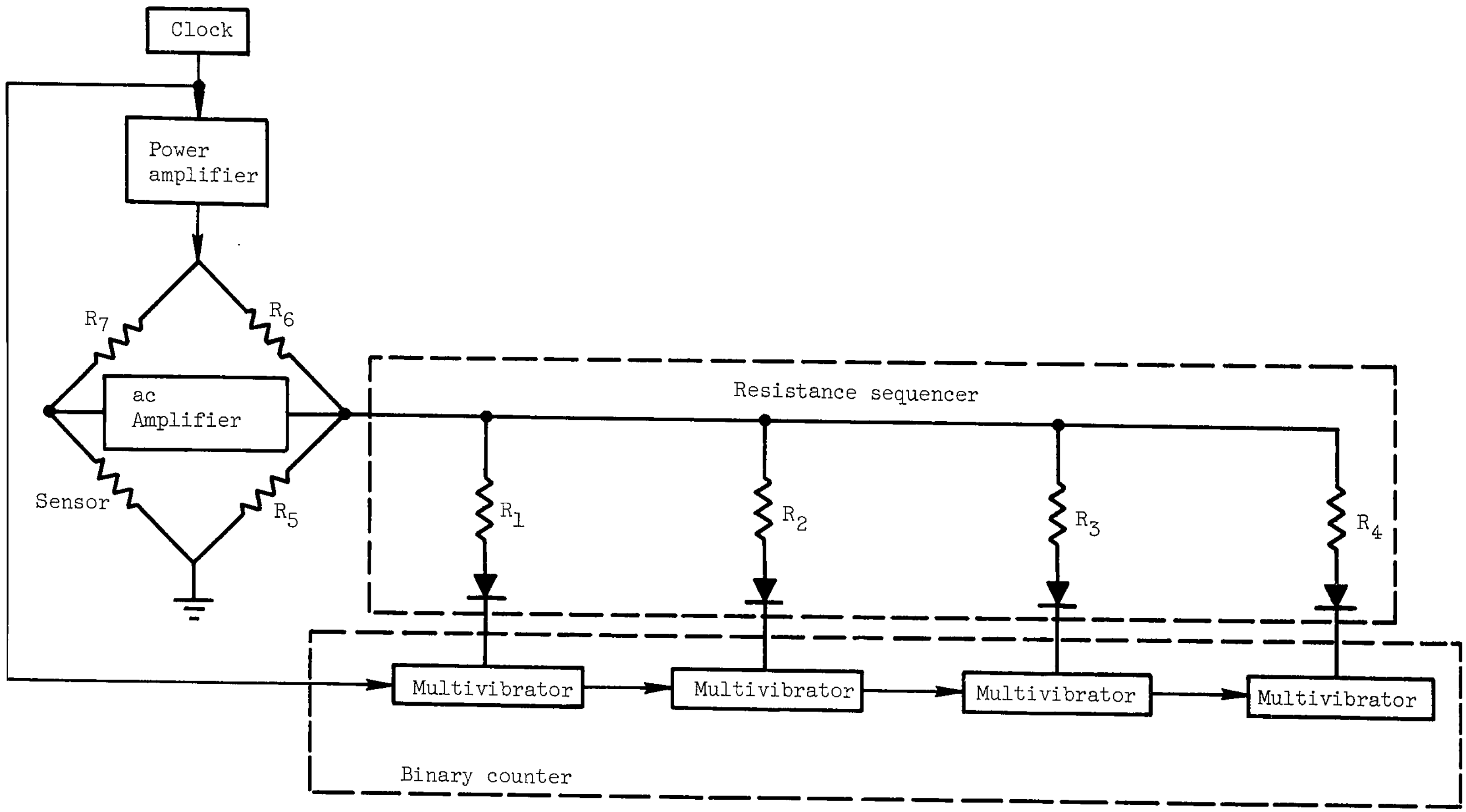

Figure 3. - Diagram illustrating resistance sequencer method.

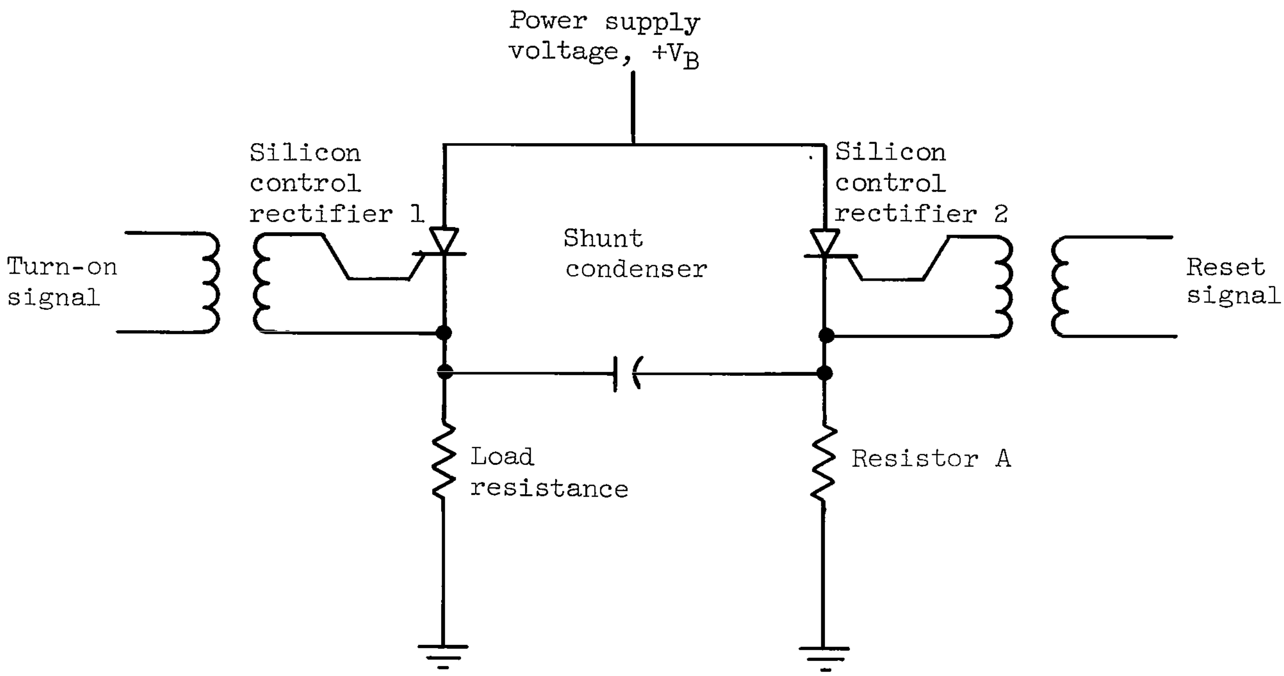

Figure 4. - Conventional switching circuit.

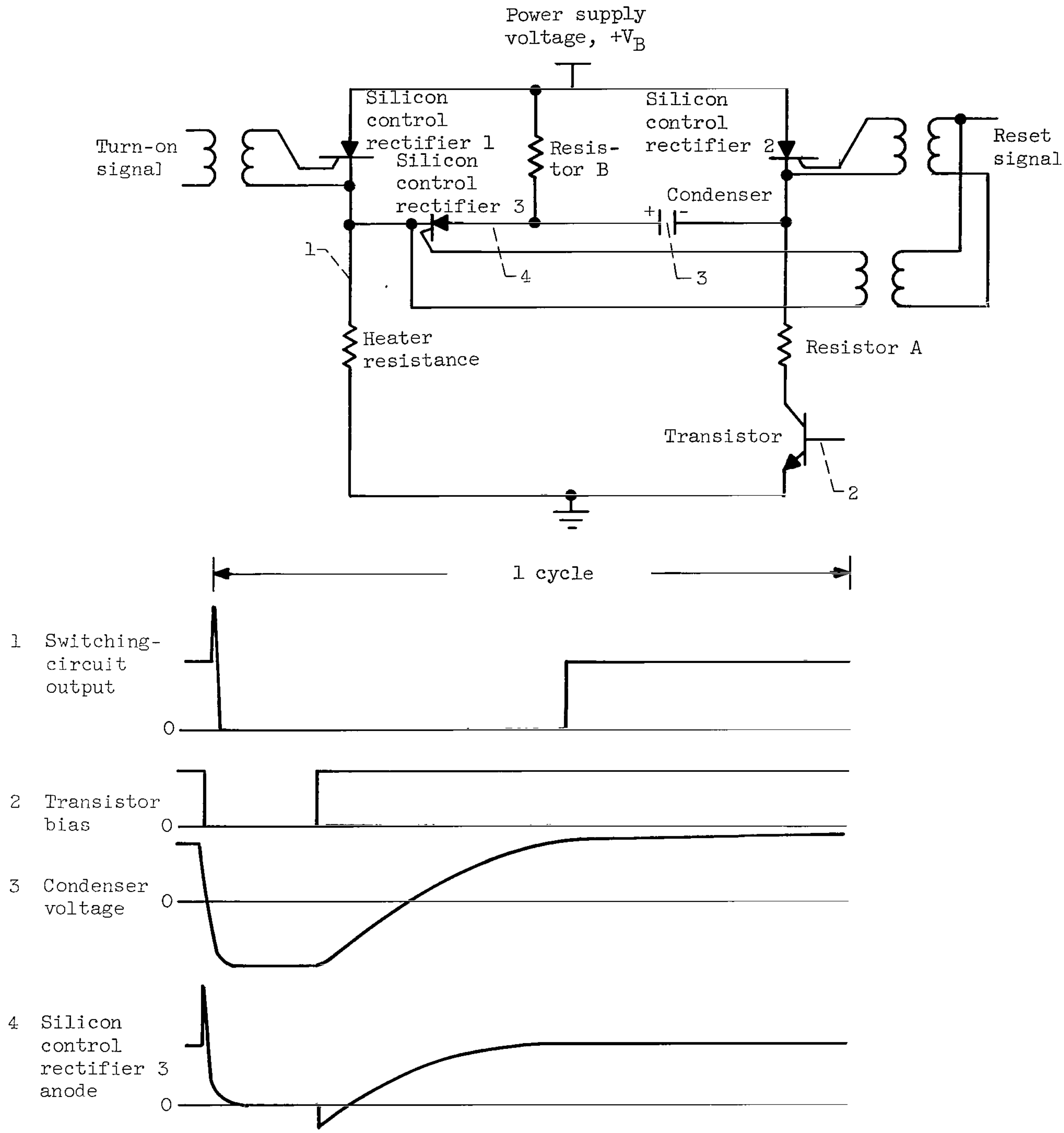

Figure 5. - Modified switching circuit and sequence diagram.

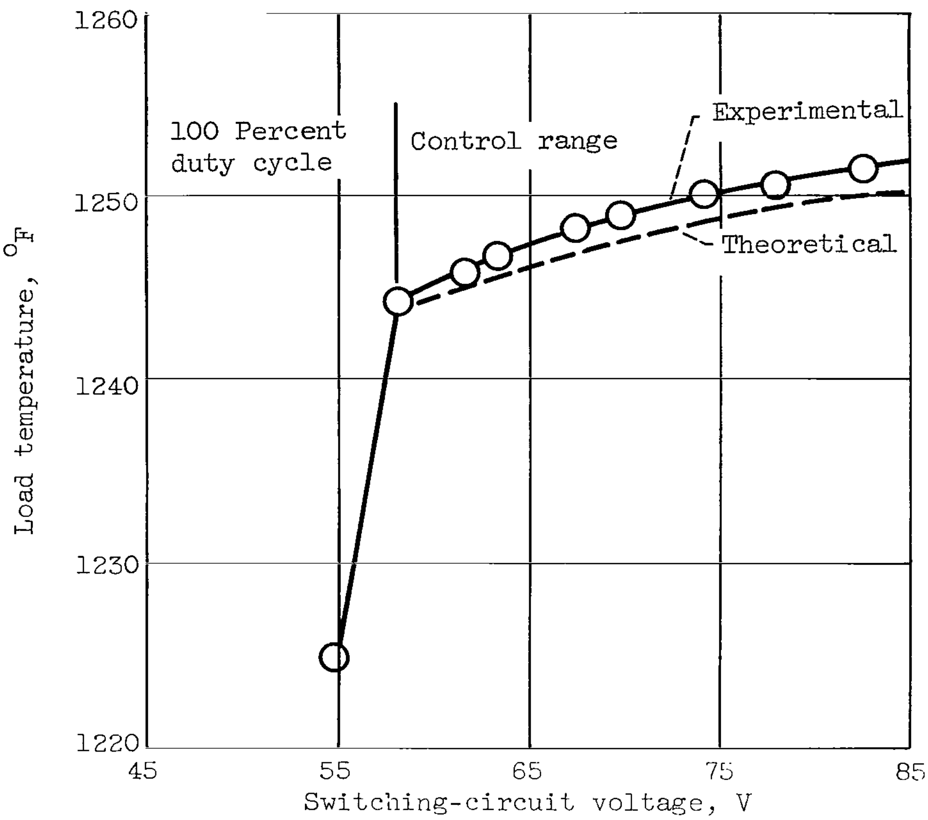

Figure 6. - Load temperature as function of switching-circuit voltage.

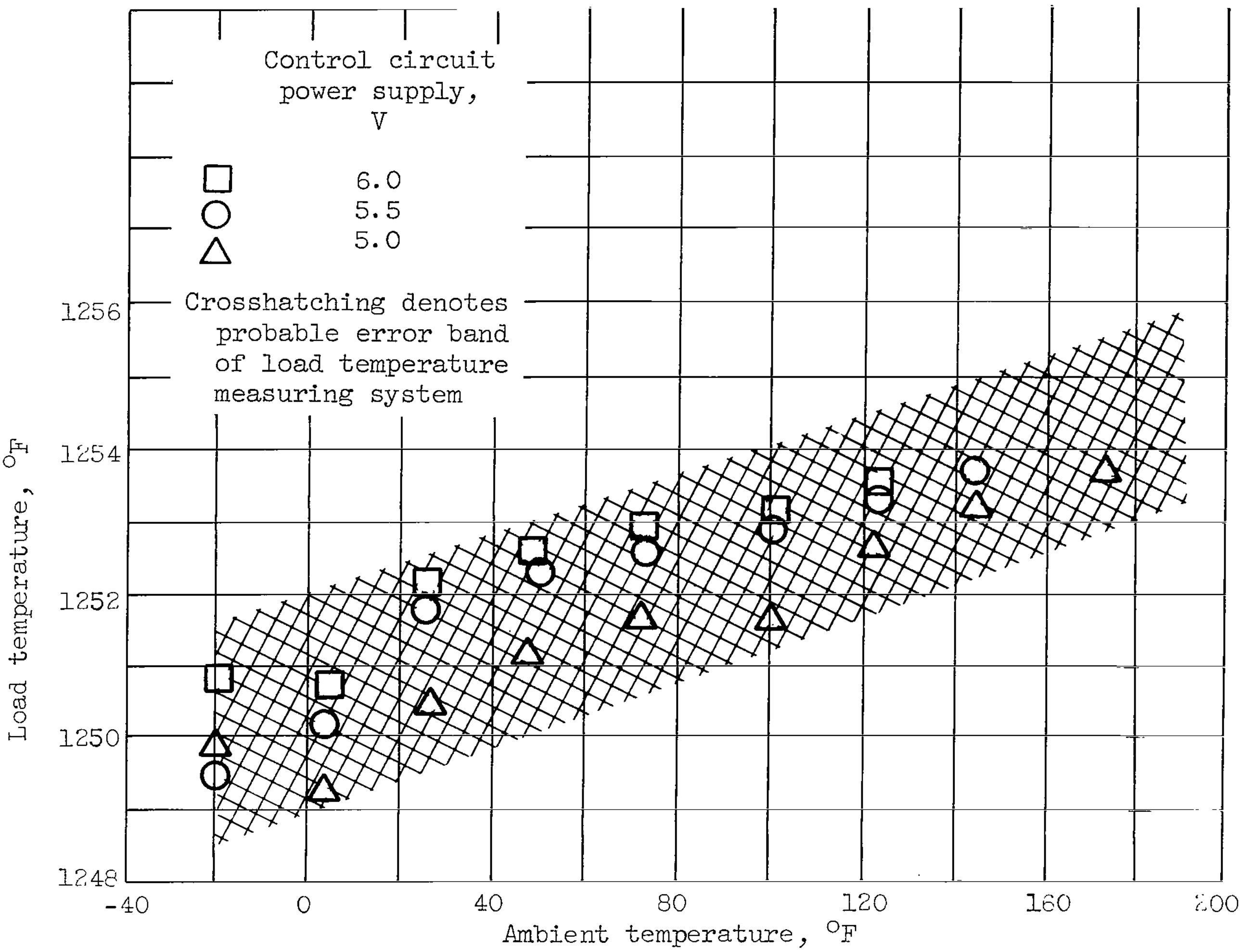

Figure 7. - Ambient temperature of control circuit as function of load temperature.

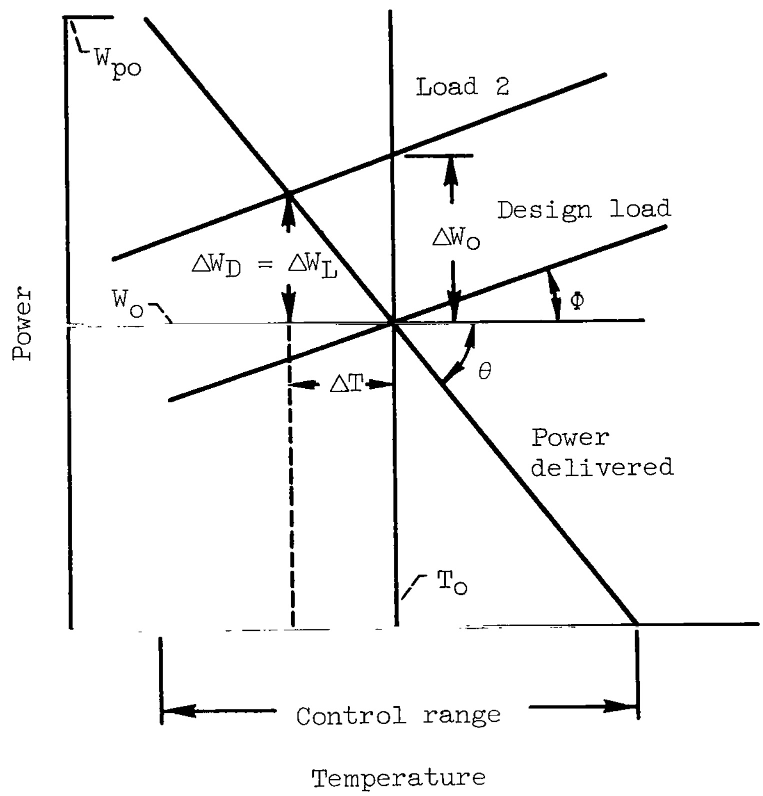

Figure 8. - Effect of load change on load temperature.

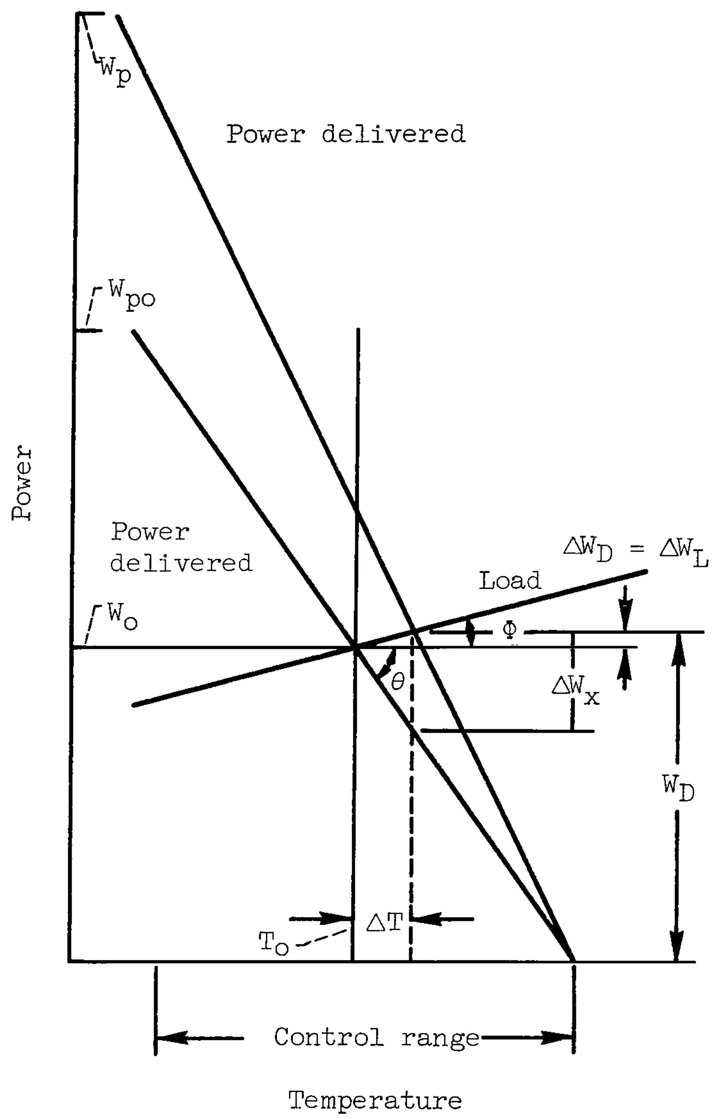

Figure 9. - Effect of switching circuit supply voltage change on load temperature.

NASA-Langley, 1966 E-3118

"The aeronautical and space activities of the United States shall be conducted so as to contribute . . . to the expansion of human knowledge of phenomena in the atmosphere and space. The Administration shall provide for the widest practicable and appropriate dissemination of information concerning its activities and the results thereof."

—NATIONAL AERONAUTICS AND SPACE ACT OF 1958

NASA SCIENTIFIC AND TECHNICAL PUBLICATIONS

TECHNICAL REPORTS: Scientific and technical information considered important, complete, and a lasting contribution to existing knowledge.

TECHNICAL NOTES: Information less broad in scope but nevertheless of importance as a contribution to existing knowledge.

TECHNICAL MEMORANDUMS: Information receiving limited distribution because of preliminary data, security classification, or other reasons.

CONTRACTOR REPORTS: Technical information generated in connection with a NASA contract or grant and released under NASA auspices.

TECHNICAL TRANSLATIONS: Information published in a foreign language considered to merit NASA distribution in English.

TECHNICAL REPRINTS: Information derived from NASA activities and initially published in the form of journal articles.

SPECIAL PUBLICATIONS: Information derived from or of value to NASA activities but not necessarily reporting the results of individual NASA-programmed scientific efforts. Publications include conference proceedings, monographs, data compilations, handbooks, sourcebooks, and special bibliographies.

Details on the availability of these publications may be obtained from:

SCIENTIFIC AND TECHNICAL INFORMATION DIVISION

NATIONAL AERONAUTICS AND SPACE ADMINISTRATION

Washington, D.C. 20546